

Semi-supervised MIMO Detection Using Cycle-consistent Generative Adversarial Network

Hongzhi Zhu, Yongliang Guo, Wei Xu*, *Senior Member, IEEE*, and Xiaohu You*, *Fellow, IEEE*,

Abstract—In this paper, a new semi-supervised deep MIMO detection approach using a cycle-consistent generative adversarial network (cycleGAN) is proposed, which performs the detection without any prior knowledge of underlying channel models. Specifically, we propose the cycleGAN detector by constructing a bidirectional loop of least squares generative adversarial networks (LS-GAN). The forward direction of the loop learns to model the transmission process, while the backward direction learns to detect the transmitted signals. By optimizing the cycle-consistency of the transmitted and received signals through this loop, the proposed method is able to train a specific detector block-by-block to fit the operating channel. The training is conducted online, including a supervised phase using pilots and an unsupervised phase using received payload data. This semi-supervised training strategy weakens the demand for the scale of labelled training dataset, which is related to the number of pilots, and thus the overhead is effectively reduced. Numerical results show that the proposed semi-blind cycleGAN detector achieves better bit error-rate (BER) than existing semi-blind deep learning detection methods as well as conditional linear detectors, especially when nonlinear distortion of the power amplifiers at the transmitter is considered.

Index Terms—cycleGAN, semi-blind MIMO detection, deep learning, semi-supervised learning, nonlinearity mitigation.

I. INTRODUCTION

Multiple-input multiple-output (MIMO) wireless communication system has promised significant enhancements over traditional single-antenna communication systems in terms of channel capacity and energy efficiency [1], [2]. While MIMO improves the performance by extending dimensions that account for time and frequency resources, it comes with new challenges of signal detection with reduced overhead to ensure reliable and efficient communications. Since signal detection is an NP-complete problem of which the optimal solution can hardly be obtained in practice, there has been growing need for low-complexity sub-optimal detection algorithms [3].

In recent years, deep learning (DL) methods have achieved great success in various fields of engineering, suggesting a new paradigm to explore data driven DL approaches for signal detection [4]. Existing DL detection methods commonly requires a large number of training data, which thereby leads to high overhead. One way to overcome this drawback is to use off-line training. However, since off-line training has

to use data from various channel realizations to obtain a general model, the off-line trained models are significantly outperformed by same models trained only with signals from the operating channel [29].

In this paper, an online trained DL detection method using cycle-consistent generative adversarial network (cycleGAN) is proposed for semi-blind MIMO detection, which outperforms typical sub-optimal detection methods with reduced overhead of pilots.

A. Classic MIMO Detection Methods

Signal detector is an important module in MIMO communication systems to estimate the transmitted signal from a corrupted and noisy version observed at the receiver. The maximum likelihood (ML) detector is known as the optimal detection method in terms of minimizing joint probability of error [5]–[7]. However, for most cases, the computational complexity of ML detector is too high to be practical, especially for high dimensional MIMO systems. Hence, there has been much interest in developing sub-optimal detection algorithms which balance performance with acceptable computational complexity. A majority of standard researches on MIMO detection have focused on linear methods, i.e. the matched filter (MF) detector [8], the zero-forcing (ZF) detector [9], and the linear minimum mean-squared error (LMMSE) detector [9]–[11]. While such linear methods indicate relatively low computational complexity, they typically require accurate channel estimation and known statistical characteristics of noise. For complex scenarios like communications with nonlinear distortion or where the channel models are mathematically intractable, the performance of linear detection methods degrades considerably [12].

B. DL-Based MIMO Detection

While classic detection algorithms are typically based on detection theory which essentially depends on the assumption of a prior probabilistic model of the transmission process, DL-based detection methods require no prior knowledge of the underlying channel model and learn the transmission process by minimizing the statistic loss function with known samples of signals. To be specific, for DL methods the signal detection problem is equivalent to a classification problem which outputs a soft decision for a given noisy and corrupted version of the desired signal.

DL models can learn directly from data and thus have a promising potential for processing transmissions under complex scenarios which can not be explicitly modeled by

H. Zhu is with the Southeast University, Nanjing, 210096, China (email: hz-zhu@seu.edu.cn);

Y. Guo is with the Purple Mountain Laboratories, Nanjing, 210096, China (email: guoyongliang@pmlabs.com.cn);

W. Xu and X. You are with the Southeast University, Nanjing, 210096, China, and the Purple Mountain Laboratories, Nanjing, 210096, China (email: {wxu, xhyu}@seu.edu.cn). They are also the corresponding authors of this paper.

mathematical expressions and where the channel models are unknown [29]. In [14], a deep MIMO detection method, DetNet, based on deep neural network (DNN) was proposed as an early attempt. While DetNet shows noticeable robustness with low computational complexity under ill-conditioned channels, it still requires instantaneous channel state information (CSI) and its performance degrades if this CSI estimate is inaccurate. In [15], a modified DNN-based detector was proposed which markedly outperforms not only DetNet but also similarly-structured detector based on convolutional neural network (CNN). However like the DetNet, the proposed DNN-based detector also requires accurate CSI estimation, which can incur extra overhead.

To avoid performance degradation caused by inaccurate CSI estimation, more complex DL models have been explored for blind or semi-blind signal detection. In [16], a blind channel equalizer based on variational autoencoder (VAE), VAEBCE, was proposed, which achieves BER performance close to non-blind adaptive LMMSE equalizer. VAEBCE models the transmission process without CSI estimation but it requires a large amount of training data which means it has to work under fixed channel to obtain enough data examples. A modified turbo equalizer, (turbo VAE), was later devised in [17] which achieves better performance than turbo Expectation-Maximization (EM) algorithm under both linear and nonlinear channels, but still requires the channel to remain unchanged.

Actually the channel changes in time and it is impractical to obtain a large scale of training dataset under a specific channel before detection. Therefore, off-line trained DL methods have been designed for practical use. Such methods can be trained off-line with data generated by simulations or collected by experiments if the underlying channel model is known and then be used for real-time signal detection as a general model. In [18], a DL-based joint channel estimation and signal detection algorithm for OFDM system was proposed, which achieved superior performance compared with conventional methods, using a deep network, CENet, for channel estimation and another deep network, CCRNet, for signal detection. However, the CENet and CCRNet indicate urgent requirement for a large training dataset and their performance degrades even for high signal-to-noise ratio (SNR) if signals under the operating SNR are not included in the training dataset. In [19], a novel compressed sensing (CS) approach using Wasserstein generative adversarial network (WGAN) was explored to conduct high dimensional channel estimation, which achieved a significant performance gain over typical techniques for sparse signal recovery such as orthogonal matching pursuit (OMP) algorithm and approximate message passing (AMP) algorithm. However, when comparing to models with same structure but trained only with signals from the operating channel, these off-line trained methods are typically outperformed.

To better conduct signal detection under channels which are completely unknown or are difficult to be derived analytically, one possible way is to explore online-trained methods which can adapt themselves to the operating channel with reduced overhead.

C. Contributions

Since standard detection methods may face difficulty when the underlying channel model is unknown and when the operating channel is hard to be tracked with reduced overhead, the best approach to designing detection algorithms which can address such issues remains to be explored. In this paper, we propose a novel semi-blind MIMO signal detection method using cycleGAN, which is trained online using the current pilots and received payload data to keep tracking the changing channels. The major contributions of our work are summarized as follows:

- The cycleGAN detector requires neither prior knowledge of the channel nor prior simulation data for off-line training. It performs well even when the underlying channel model is unknown and when there are unknown effects in the transmission such as nonlinear distortion due to imperfect power amplifiers.
- Different from typical DL detection methods which require large overhead for training data and have to be trained off-line for general use, the number of pilots needed to train the cycleGAN detector is no more than the number of transmit antennas as the popular setup in practice, and the cycleGAN detector does not require explicit CSI estimation, which further reduces the overhead.
- We propose a bidirectional network loop for the cycleGAN detector to check the cycle-consistency of signals, where the received payload data are also be used to train the model in an unsupervised way. The detection accuracy is therefore improved and the overfitting caused by the lack of training data is efficiently avoided.

Numerical results show that the BER performance achieved by the cycleGAN detector is significantly better than that achieved by the non-blind LMMSE detector and other standard semi-blind DL detection methods, especially for scenarios with nonlinear distortion. Further experiments also illustrate that depending on the architecture of cycleGAN, the introduction of unsupervised training with received payload data makes noticeable improvement on the BER performance than the same model trained supervisedly with pilots only.

D. Paper Outline

The rest of this paper is organized as follows. In Section II, we present the system model and state the MIMO detection problem. In Section III, the mechanism of the proposed cycleGAN detector is introduced with the training strategy. Implementation details of the cycleGAN detector is elaborated in Section IV, including the pre-processing of dataset and some empirical training tricks. The performance of the cycleGAN detector is evaluated with comparisons in Section V. Conclusions are drawn in Section VI.

II. PREREQUISITES

In this section, we introduce the MIMO communication system model and present the problem formulation of MIMO detection.

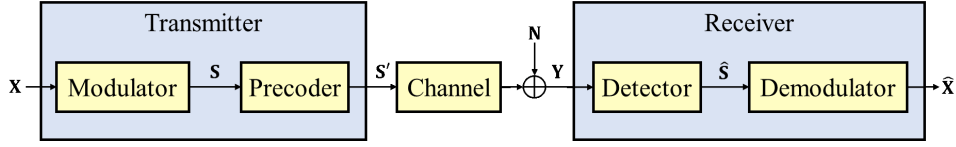


Fig. 1. MIMO downlink communication system model. The source bit sequence \mathbf{X} is modulated into \mathbf{S} and precoded into \mathbf{S}' at the transmitter. \mathbf{S}' is then passed through the channel and is received as \mathbf{Y} . At the receiver an estimation of \mathbf{S} is obtained as $\hat{\mathbf{S}}$ by a detector basing on \mathbf{Y} and is then demodulated into $\hat{\mathbf{X}}$ as a recovery of \mathbf{X} .

A. System Model

We consider the downlink of a MIMO system as shown in Fig. 1 with N_s transmit antennas and N_r receive antennas. In this figure, \mathbf{X} is the source bit sequence, \mathbf{S} is the modulated signal, and \mathbf{S}' is the precoded signal for transmission. The precoding process can be formulated as

$$\mathbf{S}' = \mathbf{F}\mathbf{S}, \quad (1)$$

where \mathbf{F} is the precoding matrix. At the receiver side, let we define \mathbf{N} as the additive noise, and \mathbf{Y} is the received signal.

The standard linear input-output relation of a MIMO communication system is given by

$$\mathbf{Y} = \mathbf{H}\mathbf{F}\mathbf{S} + \mathbf{N}, \quad (2)$$

where $\mathbf{H} \in \mathbb{C}^{N_r \times N_s}$ is the MIMO channel matrix.

However, considering nonlinear distortion in the system such as the peak-to-average power ratio reduction in OFDM systems [20], low precision ADC quantization [21], nonlinearity of power amplifiers [22], in more general scenarios (2) is reformulated by

$$\mathbf{Y} = f_{\mathbf{H}}(\mathbf{S}) + \mathbf{N}, \quad (3)$$

where $f_{\mathbf{H}}(\cdot)$ is a nonlinear function which models the entire transmission process including the precoding, physical channel, and nonlinear distortion.

The received signal \mathbf{Y} is always noisy and corrupted by the channel. Since the channel is unknown and changes in time, pilots need to be periodically inserted in the transmitted signals for the receiver to estimate the channel. The goal of the detector is to reconstruct the payload \mathbf{S} from the observed \mathbf{Y} and the pilots. After detection, the estimated $\hat{\mathbf{S}}$ is passed to the demodulator to recover the source bit sequence $\hat{\mathbf{X}}$, denoted as $\hat{\mathbf{X}}$.

B. MIMO Detection

In a typical MIMO system, signal detection is conducted after each transmission period which contains a pilot-training period and a data-sending period. We assume a block-fading scenario with time division duplex (TDD) mode and a coherence time transmitting $K = P + D$ symbols, where the first P symbols make up a pilot sequence \mathbf{S}_P and the following D symbols are the payload data \mathbf{S}_D . Accordingly, the received signal in (3) can be rewritten as

$$[\mathbf{Y}_P, \mathbf{Y}_D] = f_{\mathbf{H}}([\mathbf{S}_P, \mathbf{S}_D]) + \mathbf{N}, \quad (4)$$

where \mathbf{Y}_P and \mathbf{Y}_D are respectively the received pilots and received payload data. In the pilot-training period of P symbols,

both \mathbf{Y}_P and \mathbf{S}_P are known, which allows us to model $f_{\mathbf{H}}(\cdot)$ by a supervised training phase. In the subsequent data-sending period of D symbols, standard pilot-aided detection methods detect the payload \mathbf{S}_D directly with \mathbf{Y}_D using the previously trained model. However, for a relatively complex $f_{\mathbf{H}}(\cdot)$, since the size of \mathbf{Y}_P is limited by the number of pilot overhead, the previously trained model has a high risk of overfitting and is considered insufficiently reliable. For the proposed cycleGAN detector, we pack \mathbf{S}_P , \mathbf{Y}_P , and \mathbf{Y}_D together for an extra semi-supervised training phase so that the model is further updated to fit the payload data. After the semi-supervised training phase, the detector is used to recover the transmitted payload \mathbf{S}_D .

III. CYCLEGAN DETECTOR

In this section, we formulate the mechanism of the cycleGAN detector, including the architecture of cycleGAN and the training strategy.

A. LS-GAN

To conduct signal detection, it is necessary to setup a model to describe the relationship between the transmitted signal and the received signal (e.g., channel model and detection algorithm). Standard channel models and detection algorithms are majorly based on explicit mathematical tools, which would face difficulty on covering some unknown effects in the actual channel, thus suggesting exploration of DL models. Moreover, while conducting signal detection, the model will have to generate new signals which are not learned in the training dataset due to the limitation of pilots. Therefore, generative models can be rather preferred than some classic DL models such as basic DNN and CNN which are commonly used in classification tasks. LS-GAN is a modified version of generative adversarial network (GAN), which uses the least squares distance as the training loss instead of cross entropy, and has been proved stabler with better performance than typical generative models [23], which indicates a promising potential for MIMO detection. Note that since LS-GAN is still a supervised learning model, we set a loop of two LS-GANs as a cycleGAN later in Section III-B to introduce unsupervised learning with received payload data for further improvement.

The architecture of LS-GAN used in the cycleGAN detector is shown in Fig. 2. An LS-GAN consists of a generator $G(\cdot)$ and a discriminator $D(\cdot)$, each of which is implemented by a DNN. For each single vector of input data \mathbf{x} , $G(\cdot)$ outputs an estimated sample \mathbf{y}' , a fake sample, as

$$\mathbf{y}' = G(\mathbf{x}). \quad (5)$$

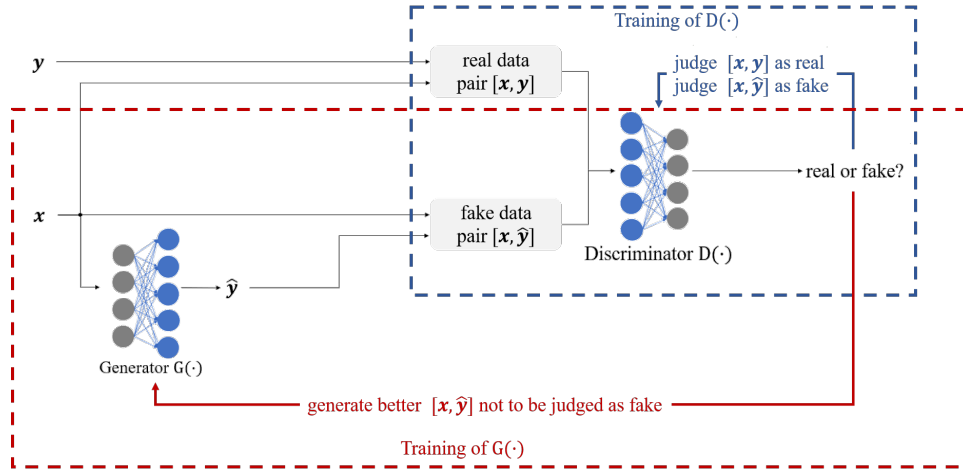


Fig. 2. Architecture of LS-GAN, consisting of a generator $G(\cdot)$ and a discriminator $D(\cdot)$. Both $G(\cdot)$ and $D(\cdot)$ are implemented by deep neural networks (DNN) and are trained under an adversarial training strategy to acquire the mapping relationship between \mathbf{x} and \mathbf{y} .

Then in order to make \mathbf{y}' an accurate estimate of the corresponding real output \mathbf{y} , we pack the fake data pair $[\mathbf{x}, \mathbf{y}']$ and the real data pair $[\mathbf{x}, \mathbf{y}]$ together to train $D(\cdot)$ for global discrimination [24]. The output of $D(\cdot)$ is a scalar which indicates whether the input data pair is real. For the LS-GAN, the expected output of $D(\cdot)$ is given by

$$D([\mathbf{x}_{\text{in}}, \mathbf{y}_{\text{in}}]) = \begin{cases} 1, & \text{if } [\mathbf{x}_{\text{in}}, \mathbf{y}_{\text{in}}] \text{ is real} \\ -1, & \text{otherwise,} \end{cases} \quad (6)$$

where $[\mathbf{x}_{\text{in}}, \mathbf{y}_{\text{in}}]$ is the input data pair. The $D(\cdot)$ is trained to judge whether \mathbf{y}' matches \mathbf{x} , subsequently guiding the training of $G(\cdot)$ since the purpose of $G(\cdot)$ is to generate an accurate estimate \mathbf{y}' to get a positive judgement from $D(\cdot)$. Then the whole system could be trained under an adversarial strategy and will finally reach Nash equilibrium, where $G(\cdot)$ has become a satisfying generator so that $D([\mathbf{x}, \mathbf{y}'])$ will be close to 0, and $D(\cdot)$ is therefore no longer able to identify whether \mathbf{y}' is real [23].

Now we give a detailed formulation of the LS-GAN model. Firstly, we focus on the mechanism of the generator $G(\cdot)$, which is realized by a DNN parameterized by θ . The input data of $G(\cdot)$ could be considered as a sample data \mathbf{x} obeying input-distribution $P_X(\mathbf{x})$, and the output of $G(\cdot)$ is considered as another sample data $G(\mathbf{x})$ obeying the generate-distribution $P_G(\mathbf{x}; \theta)$. Assuming that the real output-distribution is $P_{Y|X}(\mathbf{x})$, then the purpose of $G(\cdot)$ is equivalent to training $P_G(\mathbf{x}; \theta)$ to approximate $P_{Y|X}(\mathbf{x})$ by calculating the best parameter θ^* by

$$\theta^* = \arg \min_{\theta} \mathcal{L}_0(P_{Y|X}(\mathbf{x}) \| P_G(\mathbf{x}; \theta)), \quad (7)$$

where $\mathcal{L}_0(P_{Y|X}(\mathbf{x}) \| P_G(\mathbf{x}; \theta))$ is the least squares distance between $P_{Y|X}(\mathbf{x})$ and $P_G(\mathbf{x}; \theta)$. In fact, since the real output-distribution $P_{Y|X}(\mathbf{x})$ is unknown, $\mathcal{L}_0(P_{Y|X}(\mathbf{x}) \| P_G(\mathbf{x}; \theta))$ is represented by $\mathbb{E}[D([\mathbf{x}, G(\mathbf{x})])^2]$, where $\mathbb{E}[\cdot]$ is the expectation function, since the output of $D(\cdot)$ can be considered an approximate indicator of the distance between the generate-distribution and the real output-distribution.

Then we elaborate the mechanism of the discriminator $D(\cdot)$, which is a DNN classifier parameterized by ϕ . The training dataset of $D(\cdot)$ contains real data pairs $[\mathbf{x}, \mathbf{y}]$ and fake data pairs $[\mathbf{x}, \mathbf{y}']$ generated by $G(\cdot)$. Then the purpose of $D(\cdot)$ is equivalent to solving the binary classification problem, of which the distance between real data pair and fake data pair could be given by the squared error as

$$\mathcal{L}_1([\mathbf{x}_{\text{in}}, \mathbf{y}_{\text{in}}], z, D) = z(D([\mathbf{x}_{\text{in}}, \mathbf{y}_{\text{in}}]) - 1)^2 + (1 - z)(D([\mathbf{x}_{\text{in}}, \mathbf{y}_{\text{in}}]) + 1)^2, \quad (8)$$

where z is the data label given by

$$z = \begin{cases} 1, & \text{if } [\mathbf{x}_{\text{in}}, \mathbf{y}_{\text{in}}] \text{ is real} \\ 0, & \text{otherwise.} \end{cases} \quad (9)$$

Then we rewrite (8) by an accumulation form of N training samples:

$$\mathcal{L}_N([\mathbf{x}_i, \mathbf{y}_i], z_i)_{i=1}^N, D) = \frac{1}{N} \left[\sum_{i=1}^N z_i (D([\mathbf{x}_i, \mathbf{y}_i]) - 1)^2 + \sum_{i=1}^N (1 - z_i) (D([\mathbf{x}_i, \mathbf{y}_i]) + 1)^2 \right]. \quad (10)$$

Note that the input data of $D(\cdot)$ comes from either the real data or the fake data generated by $G(\cdot)$, which implies that (10) is actually a function of both $G(\cdot)$ and $D(\cdot)$. Therefore, we can rewrite (10) as

$$\mathcal{L}_2(G, D) = \mathbb{E}_{\mathbf{x} \sim P_X, \mathbf{y} \sim P_{Y|X}} [(D([\mathbf{x}, \mathbf{y}]) - 1)^2 + (D([\mathbf{x}, G(\mathbf{x})]) + 1)^2], \quad (11)$$

which is set as the objective function for optimizing $D(\cdot)$. Taking the derivation of $\mathcal{L}_2(G, D)$ and forcing it to zero, we obtain the optimal $D(\cdot)$ minimizing $\mathcal{L}_2(G, D)$ as

$$D^*([\mathbf{x}, \mathbf{y}]) = \frac{p_{Y|X}(\mathbf{y}) - p_G(\mathbf{y})}{p_{Y|X}(\mathbf{y}) + p_G(\mathbf{y})}, \quad (12)$$

where $p_{Y|X}$ and p_G are the probability density functions (PDF) of $P_{Y|X}$ and P_G respectively.

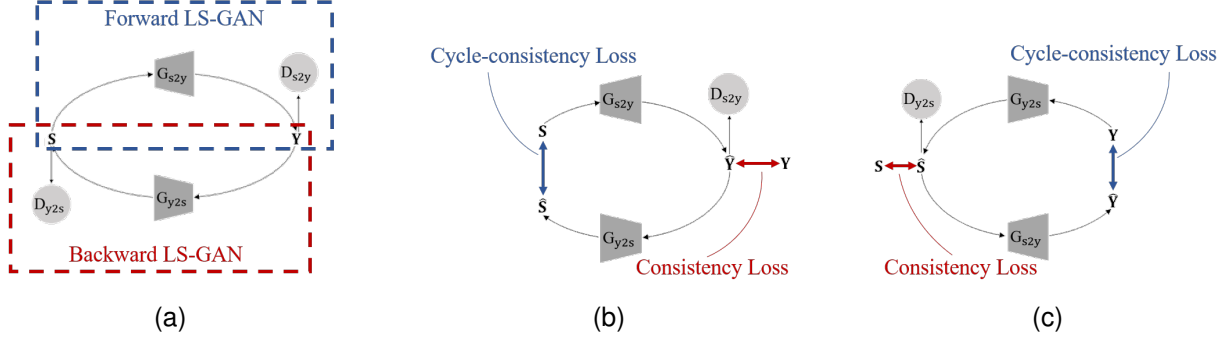


Fig. 3. (a) Architecture of the proposed cycleGAN. Two LS-GANs are coupled into a bidirectional loop so that the input data could be sent to another side and back again for checking the cycle-consistency. The cycleGAN introduces a forward loss as (b) to check the consistency in the path of $S \rightarrow Y \rightarrow S$ and a backward loss as (c) to check the consistency in the path of $Y \rightarrow S \rightarrow Y$.

Then for the perspective of $G(\cdot)$, since $P_{Y|X}(\mathbf{x})$ is unknown, we represent the least squares distance in (7) by the output of $D(\cdot)$ as

$$\mathcal{L}_0(P_{Y|X}(\mathbf{x}) \| P_G(\mathbf{x}; \boldsymbol{\theta})) \triangleq \mathbb{E}_{\mathbf{x} \sim P_X} [D([\mathbf{x}, G(\mathbf{x})])^2], \quad (13)$$

which is then set as the objective function for optimizing $G(\cdot)$. So far we have transformed the problem of solving unknown $P_{Y|X}(\mathbf{x})$ into a problem of minimizing the square expectation of $D([\mathbf{x}, G(\mathbf{x})])^2$, which yields the optimal $G^*(\mathbf{x})$ with the optimal $\boldsymbol{\theta}^*$ given by

$$\boldsymbol{\theta}^* = \arg \min_{\boldsymbol{\theta}} \mathbb{E}_{\mathbf{x} \sim P_X} [D([\mathbf{x}, G(\mathbf{x}; \boldsymbol{\theta})])^2]. \quad (14)$$

For the LS-GAN as illustrated in Fig. 2, we alternatively train $D(\cdot)$ and $G(\cdot)$ according to (11) and (14) respectively. During the training, the discriminator $D(\cdot)$ aims at minimizing $\mathbb{E}_{\mathbf{x} \sim P_X, \mathbf{y} \sim P_{Y|X}} [(D([\mathbf{x}, \mathbf{y}]) - 1)^2 + (D([\mathbf{x}, G(\mathbf{x})]) + 1)^2]$ with fixed $G(\cdot)$ so that it could be able to identify whether the input data is real, while the generator $G(\cdot)$ aims at minimizing $\mathbb{E}_{\mathbf{x} \sim P_X} [D([\mathbf{x}, G(\mathbf{x})])^2]$ with fixed $D(\cdot)$ so that the generated fake data can muddle through the discrimination.

We setup two LS-GANs to conduct signal detection, of which the forward LS-GAN models the transmission process and the backward LS-GAN models the detector. The two LS-GANs are set with similar network structures, but trained with converse input and output. The generator and the discriminator of the forward LS-GAN are denoted, respectively, by $G_{s2y}(\cdot)$ and $D_{s2y}(\cdot)$, while those of the backward LS-GAN are denoted, respectively, by $G_{y2s}(\cdot)$ and $D_{y2s}(\cdot)$. Actually, using the backward LS-GAN could be enough for detection if there is abundant training data for supervised learning. Since the number of pilots has to be limited in practice, we consider introducing extra unsupervised training with received payload data by setting up a bidirectional loop of the two LS-GANs as a cycleGAN for further improvement.

B. CycleGAN

CycleGAN was originally proposed as an image-to-image translation model, an extension of GAN, using a bidirectional loop of GANs to realize image style-conversion [25]. Since signal detection could be equivalent to a signal-to-signal

translation, the core mechanism of cycleGAN can bring some guidance for designing the detector.

As the training process of LS-GAN requires real data pairs to train $D(\cdot)$, it has to work under supervised learning. However, since the training dataset is related to the pilots that can be quite limited, we consider using the received payload data for unsupervised learning to avoid overfitting and improve the detection performance. Thus, we introduce the architecture of cycleGAN to realize unsupervised training by checking the cycle-consistency of the bidirectional mapping relationship between transmitted and received signals.

The proposed cycleGAN model coupled the two LS-GANs mentioned in Section III-A into a bidirectional loop as illustrated in Fig. 3(a), by which the input data could be sent to another side and back again for checking the cycle-consistency. Then in the data-sending period the whole model could be updated by optimizing the average distance between each single received payload \mathbf{y}_D from Y_D and its cycle-output $G_{s2y}(G_{y2s}(\mathbf{y}_D))$, without the correspond transmitted signal.

For a single data pair $[s, \mathbf{y}]$, besides the basic loss function of LS-GAN in (11) and (14), we additionally introduce a forward loss as shown in Fig. 3(b) and a backward loss as shown in Fig. 3(c) to train the cycleGAN, each of which contains a consistency loss and a cycle-consistency loss.

We first evaluate the forward LS-GAN, which models the transmission process. The consistency loss is aimed at that the output estimated received signals should be consistent with the corresponding real ones, while the cycle-consistency loss is aimed at that, if using the output estimated received signals as the input of the backward LS-GAN, the new output should be consistent with the original real transmitted signals. Accordingly, we can formulate the forward loss as

$$\mathcal{L}_{fw} = \alpha \|G_{s2y}(s) - \mathbf{y}\|_1 + \beta \|G_{y2s}(G_{s2y}(s)) - s\|_1, \quad (15)$$

where $\|\cdot\|_1$ is the 1-norm of the vector, and α and β are the hyperparameters indicating the weights of the consistency loss and the cycle-consistency loss, respectively.

Analogously for the backward LS-GAN, which models the detector, mapping the received signals to corresponding transmitted signals, the consistency loss and the cycle-consistency

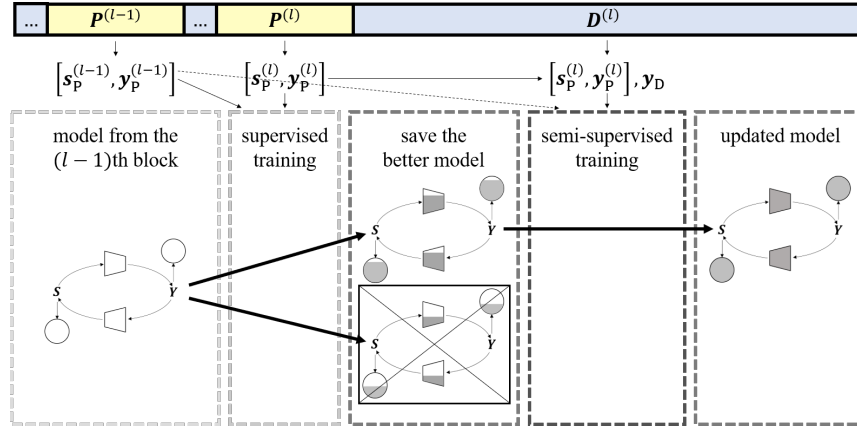


Fig. 4. Training strategy of the model for the l th block of $K = P + D$ time slots. In the pilot-training period the pilots $[s_P^{(l)}, y_P^{(l)}]$ are used for a supervised training phase. Then in the data-sending period both the pilots $[s_P^{(l)}, y_P^{(l)}]$ and received payload data y_D are used for a semi-supervised training phase. The previous pilots $[s_P^{(l-1)}, y_P^{(l-1)}]$ are also used for training if they could make the model a progress.

loss are set under similar principle with just converse input and output. Thus the backward loss is given by

$$\mathcal{L}_{bw} = \gamma \|G_{y2s}(\mathbf{y}) - \mathbf{s}\|_1 + \delta \|G_{s2y}(G_{y2s}(\mathbf{y})) - \mathbf{y}\|_1, \quad (16)$$

where γ and δ are hyperparameters indicating the weights of the subordinated loss terms.

C. Training Strategy

As illustrated in Fig. 4, for each block of $K = P + D$ symbols, we conduct a supervised training phase in the pilot-training period using pilots $[s_P, y_P]$ from $[S_P, Y_P]$ and then a semi-supervised training phase in the data-sending period using both pilots $[s_P, y_P]$ and received payload data y_D . In order to further augment the training set, let $[s_P^{(l)}, y_P^{(l)}]$ be the pilots in the l th block which is the current block for processing. Then the previous pilots $[s_P^{(l-1)}, y_P^{(l-1)}]$ in the $(l-1)$ th block are also considered to be used for the training if the channel remains mostly unchanged. In fact since the channel is unknown at the receiver, whether the previous pilots are used actually depends on if they could make the model a progress after augmented to the training set. The model is updated block-by-block to keep tracking continuous block fading channels.

1) *Pilot-Training Period*: In the pilot-training period, the pilots are divided into a training dataset and a validation dataset for supervised learning. According to (11), (13), (15), and (16), the optimal D_{s2y}^* , D_{y2s}^* , G_{s2y}^* and G_{y2s}^* are obtained by calculating the optimal network parameters ϕ_{s2y}^* , ϕ_{y2s}^* , θ_{s2y}^* , and θ_{y2s}^* as follows:

$$\begin{aligned} \phi_{s2y}^* = \arg \min_{\phi_1} \{ & \mathbb{E}_{\mathbf{s}, \mathbf{y}} [(D_{s2y}([\mathbf{s}, \mathbf{y}]; \phi_1) - 1)^2 \\ & + (D_{s2y}([\mathbf{s}, G_{s2y}(\mathbf{s})]; \phi_1) + 1)^2] \}, \end{aligned} \quad (17)$$

$$\begin{aligned} \phi_{y2s}^* = \arg \min_{\phi_2} \{ & \mathbb{E}_{\mathbf{s}, \mathbf{y}} [(D_{y2s}([\mathbf{y}, \mathbf{s}]; \phi_2) - 1)^2 \\ & + (D_{y2s}([\mathbf{y}, G_{y2s}(\mathbf{y})]; \phi_2) + 1)^2] \}, \end{aligned} \quad (18)$$

$$\begin{aligned} [\theta_{s2y}^*, \theta_{y2s}^*] = \arg \min_{[\theta_1, \theta_2]} \{ & \mathbb{E}_{\mathbf{s}, \mathbf{y}} [D_{s2y}([\mathbf{s}, G_{s2y}(\mathbf{s}; \theta_1)])^2 \\ & + D_{y2s}([\mathbf{y}, G_{y2s}(\mathbf{y}; \theta_2)])^2 \\ & + \alpha_1 \|G_{s2y}(\mathbf{s}; \theta_1) - \mathbf{y}\|_1 \\ & + \beta_1 \|G_{y2s}(\mathbf{y}; \theta_2) - \mathbf{s}\|_1 \\ & + \gamma_1 \|G_{y2s}(G_{s2y}(\mathbf{s}; \theta_1); \theta_2) - \mathbf{s}\|_1 \\ & + \delta_1 \|G_{s2y}(G_{y2s}(\mathbf{y}; \theta_2); \theta_1) - \mathbf{y}\|_1 \}, \end{aligned} \quad (19)$$

where α_1 , β_1 , γ_1 , and δ_1 are the hyperparameters indicating the weights of the subordinated loss terms defined in Section III-B. In each training epoch, we first train D_{s2y} and D_{y2s} , respectively, with fixed G_{s2y} and G_{y2s} , and then train G_{s2y} and G_{y2s} jointly with fixed D_{s2y} and D_{y2s} . Since the training purposes of the discriminators and generators are diametrically opposed to each other, these modules can keep guiding their opponents in an adversarial way, i.e., stronger generators can force the discriminator to capture deeper effects included in the transmission for stricter judgment, such as the precoding and nonlinear distortion, while stronger discriminators can force the generators to better model those effects, and then generate more accurate estimates.

In fact, before the training we also conduct some pre-processing of the dataset, such as data augmentation and normalization, to improve the stability and efficiency of learning. Implementation details and empirical training tricks will be further elaborated in Section IV. Moreover, to make use of the previous pilots in the last block, we actually train the model twice parallelly. One uses the current pilots only and the other uses pilots from both the current block and the last block. After training we compare the performance of the two temporary models and save the better one. Then the saved model is set as the initial value for subsequent semi-supervised training in the data-sending period. The previous pilots are kept for training if they do make the model a progress and are discarded if they do not. Accordingly, for the l th block, the detailed supervised training algorithm is shown in **Algorithm 1**, where m is the batch size.

2) *Data-Sending Period*: In the data-sending period, we propose a semi-supervised training strategy to update the

Algorithm 1 Supervised Training in the Pilot-Training Period

Divide the pilots $[\mathbf{S}_P^{(l)}, \mathbf{Y}_P^{(l)}]$ into a training set $[\mathbf{S}_P^{\text{train}}, \mathbf{Y}_P^{\text{train}}]$ and a validation set $[\mathbf{S}_P^{\text{val}}, \mathbf{Y}_P^{\text{val}}]$.

Operate data augmentation.

$[D_{s2y}^1, D_{y2s}^1, G_{s2y}^1, G_{y2s}^1] \leftarrow [D_{s2y}, D_{y2s}, G_{s2y}, G_{y2s}]$.

Step 1: Train $[D_{s2y}, D_{y2s}, G_{s2y}, G_{y2s}]$ by $[\mathbf{S}_P^{\text{train}}, \mathbf{Y}_P^{\text{train}}]$:

for number of training iterations **do**

Sample m transmitted signals $\{\mathbf{s}_1, \mathbf{s}_2, \dots, \mathbf{s}_m\}$ in $\mathbf{S}_P^{\text{train}}$ and the received signals $\{\mathbf{y}_1, \mathbf{y}_2, \dots, \mathbf{y}_m\}$ in $\mathbf{Y}_P^{\text{train}}$.

Update D_{s2y} by ascending the stochastic gradient:

$$\nabla \frac{1}{m} \sum_{i=1}^m [(D_{s2y}([\mathbf{s}_i, \mathbf{y}_i]) - 1)^2 + (D_{s2y}([\mathbf{s}_i, G_{s2y}(\mathbf{s}_i)]) + 1)^2].$$

Update D_{y2s} by ascending the stochastic gradient:

$$\nabla \frac{1}{m} \sum_{i=1}^m [(D_{y2s}([\mathbf{y}_i, \mathbf{s}_i]) - 1)^2 + (D_{y2s}([\mathbf{y}_i, G_{y2s}(\mathbf{y}_i)]) + 1)^2].$$

Update G_{s2y} and G_{y2s} by ascending the stochastic gradient:

$$\begin{aligned} & \nabla \frac{1}{m} \sum_{i=1}^m [D_{s2y}([\mathbf{s}_i, G_{s2y}(\mathbf{s}_i)])^2 + D_{y2s}([\mathbf{y}_i, G_{y2s}(\mathbf{y}_i)])^2 + \alpha_1 \|G_{s2y}(\mathbf{s}_i) - \mathbf{y}_i\|_1 \\ & + \beta_1 \|G_{y2s}(\mathbf{y}_i) - \mathbf{s}_i\|_1 + \gamma_1 \|G_{y2s}(G_{s2y}(\mathbf{s}_i)) - \mathbf{s}_i\|_1 + \delta_1 \|G_{s2y}(G_{y2s}(\mathbf{y}_i)) - \mathbf{y}_i\|_1]. \end{aligned}$$

Check the BER performance of G_{y2s} in $[\mathbf{S}_P^{\text{val}}, \mathbf{Y}_P^{\text{val}}]$.

end for

Step 2: Train $[D_{s2y}^1, D_{y2s}^1, G_{s2y}^1, G_{y2s}^1]$ by $[(\mathbf{S}_P^{\text{train}}, \mathbf{S}_P^{(l-1)}), (\mathbf{Y}_P^{\text{train}}, \mathbf{Y}_P^{(l-1)})]$ following the same strategy in **Step 1**.

if G_{y2s}^1 performs better than G_{y2s} :

$[D_{s2y}, D_{y2s}, G_{s2y}, G_{y2s}] \leftarrow [D_{s2y}^1, D_{y2s}^1, G_{s2y}^1, G_{y2s}^1]$.

$[\mathbf{S}_P^{\text{train}}, \mathbf{Y}_P^{\text{train}}] \leftarrow [(\mathbf{S}_P^{\text{train}}, \mathbf{S}_P^{(l-1)}), (\mathbf{Y}_P^{\text{train}}, \mathbf{Y}_P^{(l-1)})]$.

end if

model. Before the training, we firstly use the initial G_{y2s} to obtain a preliminary estimation of \mathbf{s}_D denoted as $\tilde{\mathbf{s}}_D$ for each single received payload \mathbf{y}_D by

$$\tilde{\mathbf{s}}_D = G_{y2s}(\mathbf{y}_D). \quad (20)$$

Then the data pair of $[\tilde{\mathbf{s}}_D, \mathbf{y}_D]$ is used to augment the training set and the updated D_{s2y}^* , D_{y2s}^* , G_{s2y}^* and G_{y2s}^* are obtained by updating the optimal network parameters ϕ_{s2y}^* , ϕ_{y2s}^* , θ_{s2y}^* and θ_{y2s}^* as follows:

$$\begin{aligned} \phi_{s2y}^* = \arg \min_{\phi_1} \{ & \mathbb{E}_{\mathbf{y}} [(D_{s2y}([\tilde{\mathbf{s}}, \mathbf{y}]; \phi_1) - 1)^2 \\ & + (D_{s2y}([\tilde{\mathbf{s}}, G_{s2y}(\tilde{\mathbf{s}})]; \phi_1) + 1)^2] \}, \end{aligned} \quad (21)$$

$$\begin{aligned} \phi_{y2s}^* = \arg \min_{\phi_2} \{ & \mathbb{E}_{\mathbf{y}} [(D_{y2s}([\mathbf{y}, \tilde{\mathbf{s}}]; \phi_2) - 1)^2 \\ & + (D_{y2s}([\mathbf{y}, G_{y2s}(\mathbf{y})]; \phi_2) + 1)^2] \}, \end{aligned} \quad (22)$$

$$\begin{aligned} [\theta_{s2y}^*, \theta_{y2s}^*] = \arg \min_{[\theta_1, \theta_2]} \{ & \mathbb{E}_{\mathbf{y}} [D_{s2y}([\tilde{\mathbf{s}}, G_{s2y}(\tilde{\mathbf{s}}; \theta_1)])^2 \\ & + D_{y2s}([\mathbf{y}, G_{y2s}(\mathbf{y}; \theta_2)])^2 \\ & + \alpha_2 \|G_{s2y}(\tilde{\mathbf{s}}; \theta_1) - \mathbf{y}\|_1 \\ & + \beta_2 \|G_{y2s}(\mathbf{y}; \theta_2) - \tilde{\mathbf{s}}\|_1 \\ & + \gamma_2 \|G_{y2s}(G_{s2y}(\tilde{\mathbf{s}}; \theta_1); \theta_2) - \tilde{\mathbf{s}}\|_1 \\ & + \delta_2 \|G_{s2y}(G_{y2s}(\mathbf{y}; \theta_2); \theta_1) - \mathbf{y}\|_1] \}, \end{aligned} \quad (23)$$

where α_2 , β_2 , γ_2 , and δ_2 are hyperparameters indicating the weights of the subordinated loss terms. Similar to the supervised learning phase, in each training epoch, we first

train D_{s2y} and D_{y2s} , respectively, with fixed G_{s2y} and G_{y2s} , and then train G_{s2y} and G_{y2s} jointly with fixed D_{s2y} and D_{y2s} . Note that $\tilde{\mathbf{s}}_D$ is not real data, which contains some error bits that may mislead the model training. Nevertheless, such training strategy still makes sense since the error bits normally share a relatively small percentage since this model has already been trained under the supervised step in the pilot-training period. In order to further avoid the misguidance of error bits, we keep updating $\tilde{\mathbf{s}}_D$ whenever the model has a better BER performance under the validation set. Accordingly, the detailed semi-supervised training algorithm is shown in **Algorithm 2**.

The proposed training strategy leads the model to learn a bidirectional mapping relationship between the transmitted signal and the received signal. It makes sufficient use of all the current pilots, previous pilots and the received payload data. Since no prior assumption of the mapping relationship is made, the generators are guided only by the discriminators and the consistency of data, thus promising better performance if the underlying channel model is unknown. After the whole training process is completed, the G_{s2y} is considered as a DNN model of the forward transmission process and the G_{y2s} is used as the signal detector to reconstruct the desired payload data.

D. Computational Complexity Analysis

Let n be the length of the received payload data. Then the computational complexity of classic LMMSE detector is $O(n)$.

Algorithm 2 Semi-Supervised Training in the Data-Sending Period

 $\tilde{\mathbf{S}}_D \leftarrow G_{y2s}(\mathbf{Y}_D).$
 $[\mathbf{S}^{\text{train}}, \mathbf{Y}^{\text{train}}] \leftarrow [(\mathbf{S}_P^{\text{train}}, \tilde{\mathbf{S}}_D), (\mathbf{Y}_P^{\text{train}}, \mathbf{Y}_D)].$
for number of training epochs **do**

 Sample m transmitted singals $\{\mathbf{s}_1, \mathbf{s}_2, \dots, \mathbf{s}_m\}$ in $\mathbf{S}^{\text{train}}$ and the received singals $\{\mathbf{y}_1, \mathbf{y}_2, \dots, \mathbf{y}_m\}$ in $\mathbf{Y}^{\text{train}}$.

 Update D_{s2y} by ascending the stochastic gradient:

$$\nabla \frac{1}{m} \sum_{i=1}^m [(D_{s2y}([\mathbf{s}_i, \mathbf{y}_i]) - 1)^2 + (D_{s2y}([\mathbf{s}_i, G_{s2y}(\mathbf{s}_i)]) + 1)^2].$$

 Update D_{y2s} by ascending the stochastic gradient:

$$\nabla \frac{1}{m} \sum_{i=1}^m [(D_{y2s}([\mathbf{y}_i, \mathbf{s}_i]) - 1)^2 + (D_{y2s}([\mathbf{y}_i, G_{y2s}(\mathbf{y}_i)]) + 1)^2].$$

 Update G_{s2y} and G_{y2s} by ascending the stochastic gradient:

$$\begin{aligned} & \nabla \frac{1}{m} \sum_{i=1}^m [D_{s2y}([\mathbf{s}_i, G_{s2y}(\mathbf{s}_i)])^2 + D_{y2s}([\mathbf{y}_i, G_{y2s}(\mathbf{y}_i)])^2 + \alpha_2 \|G_{s2y}(\mathbf{s}_i) - \mathbf{y}_i\|_1 \\ & + \beta_2 \|G_{y2s}(\mathbf{y}_i) - \mathbf{s}_i\|_1 + \gamma_2 \|G_{y2s}(G_{s2y}(\mathbf{s}_i)) - \mathbf{s}_i\|_1 + \delta_2 \|G_{s2y}(G_{y2s}(\mathbf{y}_i)) - \mathbf{y}_i\|_1]. \end{aligned}$$

 Check the BER performance of G_{y2s} in $[\mathbf{S}_P^{\text{val}}, \mathbf{Y}_P^{\text{val}}]$.

 If progress of G_{y2s} is made:

 $\tilde{\mathbf{S}}_D \leftarrow G_{y2s}(\mathbf{Y}_D).$
 $[\mathbf{S}^{\text{train}}, \mathbf{Y}^{\text{train}}] \leftarrow [(\mathbf{S}_P^{\text{train}}, \tilde{\mathbf{S}}_D), (\mathbf{Y}_P^{\text{train}}, \mathbf{Y}_D)].$
end for

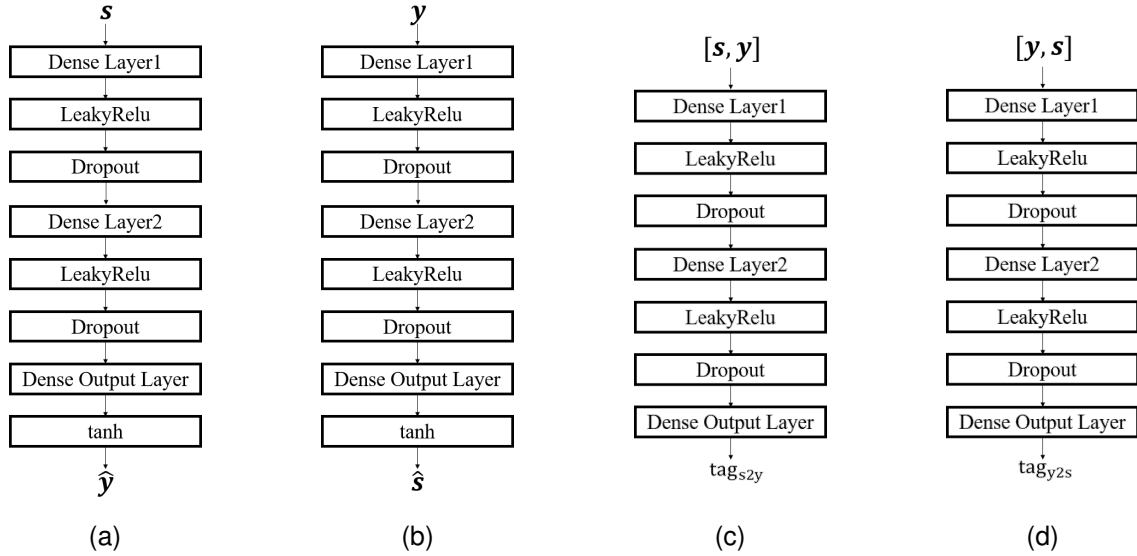


Fig. 5. (a) Architecture of G_{s2y} , where $\hat{\mathbf{y}}$ is the estimation of the received signal correspond to the input transmitted signal \mathbf{s} . (b) Architecture of G_{y2s} , where $\hat{\mathbf{s}}$ is the estimation of the transmitted signal correspond to the input received signal \mathbf{y} . (c) Architecture of D_{s2y} , where tag_{s2y} is a scalar judging whether the input data pair $[\mathbf{s}, \mathbf{y}]$ is real. (d) Architecture of D_{y2s} , where tag_{y2s} is a scalar judging whether the input data pair $[\mathbf{y}, \mathbf{s}]$ is real.

For the cycleGAN detector, the forward-pass computational complexity of the detector G_{y2s} is also $O(n)$. Note that beside the forward-pass calculation, the actual time cost also depends on the training process and the time complexity of the cycleGAN model is $O(N_r^2 n^2)$. To overcome this drawback, we set the model trained in the last block as the initial value for the next block, so that the previous knowledge can be kept to help future learning. Generally in our experiments for

each block the required number of training epochs is no more than 5000 and for successive blocks that the channel remains unchanged, the model trains about twice faster.

IV. IMPLEMENTATION DETAILS

In this section we introduce the implementation details of the cycleGAN detector. Our experiments are conducted under conda 4.9.2, python 3.8.5, and pytorch 1.11.0, where

TABLE I
AN OVERVIEW OF NETWORK CONFIGURATIONS AND PARAMETERS

	G_{s2y}	G_{y2s}	D_{s2y}	D_{y2s}
Input layer	16	16	32	32
Layer 1	Dense 256	Dense 256	Dense 512	Dense 512
Layer 2	LeakyRelu($\alpha = 0.2$)	LeakyRelu($\alpha = 0.2$)	LeakyRelu($\alpha = 0.2$)	LeakyRelu($\alpha = 0.2$)
Layer 3	Dropout(0.1)	Dropout(0.1)	Dropout(0.1)	Dropout(0.1)
Layer 4	Dense 512	Dense 512	Dense 256	Dense 256
Layer 5	LeakyRelu($\alpha = 0.2$)	LeakyRelu($\alpha = 0.2$)	LeakyRelu($\alpha = 0.2$)	LeakyRelu($\alpha = 0.2$)
Layer 6	Dropout(0.1)	Dropout(0.1)	Dropout(0.1)	Dropout(0.1)
Output layer	Dense 16-tanh	Dense 16-tanh	Dense 1	Dense 1

python is the coding language, conda is the environment for implementations of functions, pytorch is a common framework to develop DL models. In our experiments we set $N_s = 64$, $N_T = 8$, $K = 320$, $P = 64$, and $D = 256$.

A. Network Parameters

1) *Generators*: G_{s2y} and G_{y2s} are DNNs including 2 dense hidden layers and 1 dense output layer each as illustrated in Fig. 5(a) and Fig. 5(b), respectively. The input layer has 16 neurons. The first hidden layer has 256 neurons and the second hidden layer has 512 neurons. Each hidden layer follows an activation layer of ‘LeakyRelu’, with $\alpha = 0.2$ as the slope in negative-half-axis. Besides, we set a dropout layer at the end of each hidden layer to resist overfitting [26], [27], with the dormancy rate of 0.1. The output layer has 16 neurons, after which follows an activation layer of ‘tanh’. All the network parameters are regularized by L2 regularizer.

2) *Discriminators*: D_{s2y} and D_{y2s} are DNNs including 2 dense hidden layers and 1 dense output layer each as illustrated in Fig. 5(c) and Fig. 5(d), respectively. The input layer has 32 neurons. The first hidden layer has 512 neurons and the second hidden layer has 256 neurons. Each hidden layer follows an activation layer of ‘LeakyRelu’, with $\alpha = 0.2$ as the slope in negative-half-axis. Besides, we set a dropout layer at the end of each hidden layer to resist overfitting, with the dormancy rate of 0.1. The output layer has 1 neuron, the discriminator of LS-GAN does not need an activation layer at the output side [23]. All the network parameters are regularized by L2 regularizer.

The layout of the four networks we used are given in Table I. After setting up the four modules, we couple them for the cycleGAN proposed in Section III-B.

B. Pre-Processing

Pre-processing of the dataset is necessary to ensure a stable training. Our pre-processing mainly includes data augmentation, signal flattening, and normalization.

1) *Data Augmentation*: Note that the scale of pilots is limited, which may not be enough for training the model and indicates a high risk of overfitting. Thus, we consider about adding white noise for data augmentation to obtain a larger training set and a larger validation set.

The mapping of data augmentation by adding white noise is given by

$$\begin{cases} \mathbf{s}_{\text{aug}} = \mathbf{s} + \mathbf{n}_s \\ \mathbf{y}_{\text{aug}} = \mathbf{y} + \mathbf{n}_y, \end{cases} \quad (24)$$

where \mathbf{s}_{aug} and \mathbf{y}_{aug} are the augmented signals, \mathbf{s} and \mathbf{y} are the real signals, and \mathbf{n}_s and \mathbf{n}_y are the noise added for augmentation.

The number of pilots is equal to N_s . We divided the 64 pilot symbols into a training set of 48 symbols and a validation set of 16 symbols, and then augmented each dataset by 10 times for supervised training. The payload data of 256 symbols is augmented by 5 times and is packed with the training set for semi-supervised training. The original payload data of 256 symbols is used as the test set.

2) *Signal Flattening*: As it is computationally complex for neural networks to operate plural calculation in training, we flattened the complex signals into real signals, the mapping of flattening is given by:

$$\begin{cases} \mathbf{s}_{i,2k}^{\text{flt}} = \text{Re}(\mathbf{s}_{i,k}) \\ \mathbf{s}_{i,2k+1}^{\text{flt}} = \text{Im}(\mathbf{s}_{i,k}) \\ \mathbf{y}_{i,2k}^{\text{flt}} = \text{Re}(\mathbf{y}_{i,k}) \\ \mathbf{y}_{i,2k+1}^{\text{flt}} = \text{Im}(\mathbf{y}_{i,k}), \end{cases} \quad (25)$$

where $\mathbf{s}_{i,2k}^{\text{flt}}$ and $\mathbf{s}_{i,2k+1}^{\text{flt}}$ are the flattened transmitted signals, $\mathbf{y}_{i,2k}^{\text{flt}}$ and $\mathbf{y}_{i,2k+1}^{\text{flt}}$ are the flattened received signals, $\text{Re}(\cdot)$, $\text{Im}(\cdot)$ are the real part and the imaginary part of the plural respectively, $\mathbf{s}_{i,k}$, $\mathbf{y}_{i,k}$ are the original signals, i is the index of frame, and k is the index of position. After the signal flattening, the mapping between complex signals is transformed into the mapping between real signals, which is feasible to be learned by neural networks.

3) *Normalization*: Typically, while constructing a neural network, an activation function is set at the output side of each layer to introduce nonlinearity so that the network could approach complex nonlinear mapping relationships. Note that generally activation functions are sensitive only for arguments near zero, thus we adopted normalization for the flattened signals to set the numeric values between $[-1, 1]$. The mapping

TABLE II
TRAINING PARAMETERS

Training optimizer	Learning rate	Exponential decay rate	Batch size	Probability of label invert	Early stopping patience
Adam	0.0002	(0.5, 0.99)	128	5%	100 epochs

of normalization is given by:

$$\begin{cases} \mathbf{s}_{i,k}^{\text{norm}} = \frac{\mathbf{s}_{i,k}^{\text{flt}}}{\max_{1 \leq n \leq K} \{|\mathbf{s}_{n,k}^{\text{flt}}|\}} \\ \mathbf{y}_{i,k}^{\text{norm}} = \frac{\mathbf{y}_{i,k}^{\text{flt}}}{\max_{1 \leq n \leq K} \{|\mathbf{s}_{n,k}^{\text{flt}}|\}}, \end{cases} \quad (26)$$

where $\mathbf{s}_{i,k}^{\text{norm}}$ is the normalized transmitted signal, $\mathbf{y}_{i,k}^{\text{norm}}$ is the normalized received signal, i is the index of frame, and k is the index of position.

By such pre-processing procedures we modify the dataset into a more regular form to ensure a stable and efficient training procedure.

C. Training Procedure

After pre-processing, we then start training using the processed dataset, following the training strategy proposed in Section III-C. To improve the efficiency of training, we introduce some empirical training tricks for implementation, including batch training, label invert, and early stopping.

1) *Batch Training*: To conduct the gradient-based updates, in our experiments we use Adam as the optimizer with the learning rate of 0.0002 and exponential decay rate of (0.5, 0.99). Note that the variance of data can be quite large if we feed the whole dataset to train the model, which will cause inaccurate gradient calculation. Therefore, in order to obtain more accurate gradient, we set batch size $m = 128$ and feed a batch of data to the model rather than the whole dataset for each training iteration.

2) *Label Invert*: Sometimes the model may get stuck in local-optimal solutions if it erroneously learns some superficial features. Therefore, in practice we set a probability of 5% in each training iteration to invert the data labels, i.e. to set real signals as fake and set fake signals as real. In this way we help the model to reconsider whether the acquired knowledge is right and get out of the wrong learning direction.

3) *Early stopping*: Unlike traditional iterative algorithms having predefined stopping conditions, actually the training of cycleGAN can be terminated depending on the performance of G_{y2s} . If for several consecutive training epochs the BER performance of G_{y2s} remains unimproved, we stop the training to save time and avoid further overfitting. In our experiments we set the early stopping patience as 100 epochs.

The parameter setup in the model training phase is summarized in Table II.

V. NUMERICAL RESULTS

A. Simulation Setup

For evaluating the performance of the proposed cycleGAN detector, we consider the downlink transmission under Rayleigh block fading channel. The channel is generated by

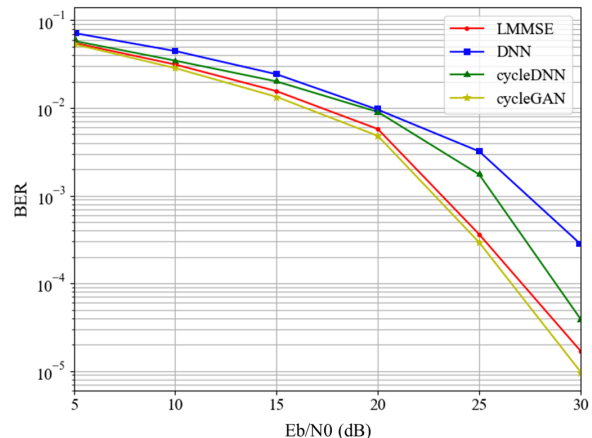


Fig. 6. BER performance of the semi-blind cycleGAN detector, the semi-blind DNN detector, the semi-blind cycleDNN detector and the non-blind LMMSE without nonlinear distortion.

the Jake's Model [28]. We assume that the CSI is perfectly estimated at the transmitter so that a precoder based on singular value decomposition (SVD) can be implemented. To assess the robustness of the detectors against nonlinear distortion, nonlinearity of power amplifiers at the transmitter is also introduced. We model the nonlinearity by $g(\mathbf{s})$ as proposed in [27]:

$$g(\mathbf{s}) = \sum_{i=1}^N a_{2i-1} \mathbf{s}^{2i-1}. \quad (27)$$

Quadrature phase shift keying (QPSK) is adopted for modulation and the additive noise is assumed white Gaussian noise.

Besides the cycleGAN detector, we also setup a typical LMMSE detector [10], a basic DNN detector [29], and a cycleDNN detector for comparison. The LMMSE detector is supposed to be non-blind, for which the SVD of the channel is also perfectly known at the receiver so that the equivalent diagonal channel matrix could be estimated for detection, indicating a quite strong prior assumption. Other detectors are supposed to be semi-blind, for which there is no extra prior knowledge except the pilots, and no pre-decoder at the receiver side. The cycleDNN detector is set by coupling only G_{y2s} and G_{s2y} into a bidirectional loop, which follows a semi-supervised training strategy similar to the cycleGAN detector without optimizing the discriminators. The DNN detector has the same architecture as the G_{y2s} but since there is no bidirectional loop, it can only be trained supervisedly with pilots.

B. BER Performance without Nonlinear Distortion

Firstly, we evaluate the BER performance of the four detectors under transmissions without nonlinear distortion. We

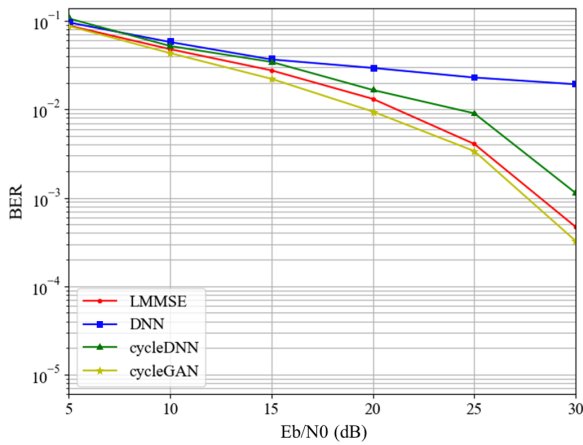


Fig. 7. BER performance of the semi-blind cycleGAN detector, the semi-blind DNN detector, the semi-blind cycleDNN detector and the non-blind LMMSE with nonlinear distortion.

compare the BER performance of the cycleGAN detector against non-blind LMMSE detector with bit signal-to-noise ratio (E_b/N_0) from 5 dB to 30 dB. For each E_b/N_0 , we generated 100 successive blocks of signals randomly, each block containing 64 symbols of pilots and 256 symbols of payload data (i.e. the overhead is 20%). For each block we train the model and calculate the BER. We record the average BER of the detectors respectively for comparison as an assessment.

Experiments demonstrate that for E_b/N_0 from 5 dB to 30 dB, as illustrated in Fig. 6, the BER performance of the cycleGAN detector stays better than other detectors and the gap between the cycleGAN detector and other detectors keeps expanding. The DNN detector performs the worst since it falls into severe overfitting due to the limitation of pilots. The cycleDNN detector performs much better than the DNN detector but since there is no guidance of discriminators, it still can not accurately model the implicit relationship between signals, such as the precoding process, thus outperformed by the non-blind LMMSE detector. The performance of the non-blind LMMSE detector is close to that of the cycleGAN detector since there is no nonlinear distortion in the transmission and the non-blind LMMSE detector has perfect knowledge of CSI.

C. BER Performance with Nonlinear Distortion

As the LMMSE detector is based on linear algorithm which may face difficulty when processing transmissions under complex scenarios, we then evaluate the robustness of the detectors against nonlinear distortion. In our experiments we set $g(s)$ in section V-A with $N = 3$, $a_1 = 1$, $a_3 = -1.5$, and $a_5 = -0.3$. Other simulation configurations are the same as in section V-B.

The BER performance of the detectors under nonlinear distortion are shown in Fig. 7. For E_b/N_0 from 5 dB to 30 dB, the DNN detector still can not overcome the overfitting and the performance of the cycleDNN detector also degrades significantly since the relationship between signals become more complex and more difficult to be captured. The performance of the cycleGAN still stays the best and the gap between the cycleGAN and the non-blind LMMSE detector is

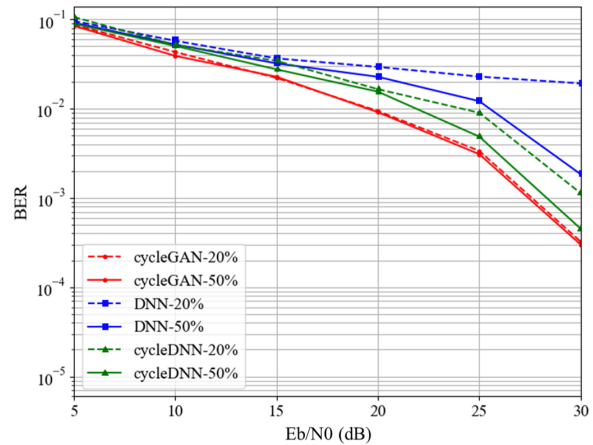


Fig. 8. BER performance of the semi-blind cycleGAN detector, the semi-blind DNN detector, and the semi-blind cycleDNN detector with 20% and 50% overhead.

further expanded than in section V-B. Note that for scenarios under low E_b/N_0 , the superiority of the cycleGAN detector over the non-blind LMMSE detector is still just passable since the risk of overfitting is quite high for DL models if there is much effect of noise in the data while only a relatively small scale of training dataset is available. But as the E_b/N_0 increases, the effect of noise is decreased so that the deep relationship between signals could be better captured, leading to better performance of the cycleGAN detector. Moreover, since neither the prior knowledge of the underlying channel model nor the CSI estimation for pre-decoding are required for the semi-blind cycleGAN detector, it indicates more practical value than the non-blind LMMSE detector.

D. Overhead Reduction

In this section we evaluate the benefit of the cycleGAN detector in reducing overhead. Since the experiments in above sections show that when the overhead is 20%, the DNN detector falls into severe overfitting and the cycleDNN detector can not accurately model the transmission process, in this section we set the overhead to 50% for the three DL detectors, i.e., increase the number of pilots to 160 symbols, and then compare the BER performance of them against those with 20% overhead. Other simulation configurations are the same as in section V-C.

The simulation results are shown in Fig. 8. Since the number of pilots is increased, the DNN detector and the cycleDNN detector can obviously better mitigate the overfitting and achieve quite lower BER than with 20% overhead. However, these two detectors still cannot outperform the cycleGAN detector with 20% overhead even with increased training data. Note that for the cycleGAN detector, the increase of overhead does not bring significant improvement since 20% overhead is already enough for the supervised training phase and the model can be further updated unsupervisedly by the received payload data even the corresponding transmitted signals are unknown. The results indicate that the cycleGAN detector can save over half of the requirement for overhead than standard DL models for similar BER performance. Such benefit in reducing the

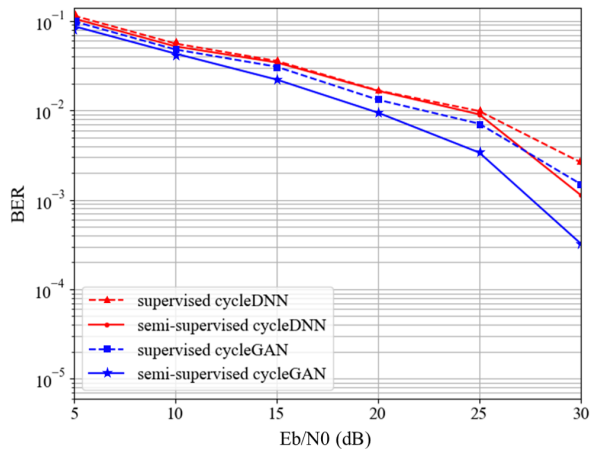


Fig. 9. BER performance of the semi-supervised cycleGAN detector, the supervised cycleGAN detector, the semi-supervised cycleDNN detector and the supervised cycleDNN detector.

overhead is mainly achieved by virtue of the guidance from discriminators and the introduction of unsupervised learning. The guidance of discriminators can help the model to better capture the deep effects in the transmission process, such as the precoding and nonlinear distortion, while the introduction of unsupervised learning can make use of the received payload data to equivalently augment the training dataset.

E. Benefit of Semi-supervised Learning

To further evaluate the benefit of semi-supervised learning, we also investigate the BER performance of the cycleGAN detector trained by semi-supervised learning and the same model trained by supervised learning with pilots only, with other simulation conditions unchanged as in V-C. Same comparison between the semi-supervised and supervised cycleDNN detector is also investigated for more general conclusion.

Fig. 9 shows that for E_b/N_0 from 5 dB to 30 dB, the BER performance of the semi-supervised cycleGAN detector stays better than the supervised cycleGAN detector with over 10% less BER, and the semi-supervised cycleDNN detector also outperforms the supervised cycleDNN detector especially for high E_b/N_0 . Note that the benefit of semi-supervised learning for the cycleDNN detector is relatively limited since there is no guidance from discriminators so that it can be more difficult to avoid mislead of error bits in the unsupervised learning. Both the cycleGAN detector and the cycleDNN detector show the benefit of semi-supervised learning since plenty of new knowledge is provided by the received payload data during unsupervised learning, by which the model is able to better capture the distortion and other deep effects in the transmission process. Actually, the performance of the supervised cycleGAN detector is even worse than the non-blind LMMSE detector since the limited pilots do cause serious overfitting, and the semi-supervised learning makes great contributions to overcome this drawback.

VI. CONCLUSION

A semi-blind MIMO detection method based on cycleGAN is proposed, which couples two LS-GANs into a bidirec-

tional loop to model the transmission process by optimizing the cycle-consistency. We trained the model under a semi-supervised learning strategy to make sufficient use of both the pilots and the received payload data. Numerical results show that the BER performance of the cycleGAN detector has a great superior over that of the non-blind LMMSE detector and other semi-blind standard DL detection methods, especially when processing downlink transmission with nonlinear distortion. Another motivation of the cycleGAN detector over standard downlink detection algorithms is that the cycleGAN detector is entirely data driven and does not require neither the prior assumption of the underlying channel model nor the CSI estimation for pre-decoding, indicating reduced overhead and more promising application prospect for practical use.

REFERENCES

- [1] H. Q. Ngo, A. Ashikhmin, H. Yang, E. G. Larsson, and T. L. Marzetta, "Cell-free massive MIMO versus small cells," *IEEE Trans. Wireless Commun.*, vol. 16, no. 3, pp. 1834–1850, Mar. 2017.
- [2] S. Buzzi and C. D'Andrea, "Cell-free massive MIMO: User-centric approach," *IEEE Wireless Commun. Lett.*, vol. 6, no. 6, pp. 706–709, Dec. 2017.
- [3] N. Samuel, T. Diskin, and A. Wiesel, "Learning to detect," 2018, arXiv:1805.07631.
- [4] M. Zamanipour, "A survey on deep-learning based techniques for modeling and estimation of massive MIMO channels," 2019, arXiv:1909.05148.
- [5] M. Ghosh and C. L. Weber, "Maximum-likelihood blind equalization," *Opt. Eng.*, vol. 31, no. 6, pp. 1224–1229, 1992.
- [6] L. Tong and S. Perreau, "Multichannel blind identification: From subspace to maximum likelihood methods," in *Proc. IEEE*, vol. 86, no. 10, pp. 1951–1968, Oct. 1998.
- [7] H. A. Cirpan and M. K. Tsatsanis, "Maximum likelihood blind channel estimation in the presence of doppler shifts," *IEEE Trans. Signal Process.*, vol. 47, no. 6, pp. 1559–1569, Jun. 1999.
- [8] Y. Hama and H. Ochiai, "Performance analysis of matched filter detector for MIMO systems in Rayleigh fading channels," in *Proc. IEEE Global Commun. Conf.*, Singapore, 2017, pp. 1–6.
- [9] A. Trimeche, N. Boukid, A. Sakly, and A. Mtibaa, "Performance analysis of ZF and MMSE equalizers for MIMO systems," in *Proc. 7th Int. Conf. Design Technol. Integr. Syst.*, 2012, pp. 1–6.
- [10] N. Kim, Y. Lee, and H. Park, "Performance analysis of MIMO system with linear MMSE receiver," *IEEE Trans. Wireless Commun.*, vol. 7, no. 11, pp. 4474–4478, Nov. 2008.
- [11] Y. Gong, X. Hong, and K. F. Abu-Salim, "Adaptive MMSE equalizer with optimum tap-length and decision delay," in *Proc. Sensor Signal Process. Defence (SSPD)*, 2010, pp. 1–5.
- [12] S. Chen, S. X. Ng, E. F. Khalaf, A. Morfeq, and N. D. Alotaibi, "Multiuser detection for nonlinear MIMO uplink," *IEEE Trans. Commun.*, vol. 68, no. 1, pp. 207–219, Jan. 2020.
- [13] N. Farsad and A. Goldsmith, "Neural network detection of data sequences in communication systems," *IEEE Trans. Signal Process.*, vol. 66, no. 21, pp. 5663–5678, Nov. 2018.
- [14] N. Samuel, T. Diskin, and A. Wiesel, "Deep MIMO detection," in *Proc. IEEE 18th Int. Workshop Signal Process. Advances Wireless Commun.*, Jul. 2017.
- [15] Q. Chen, S. Zhang, S. Xu, and S. Cao, "Efficient MIMO detection with imperfect channel knowledge – A deep learning approach," 2019, arXiv:1903.07831.
- [16] A. Caciularu and D. Burshtein, "Blind channel equalization using variational autoencoders," in *Proc. IEEE Int. Conf. Commun. Workshops*, May. 2018.
- [17] A. Caciularu and D. Burshtein, "Unsupervised linear and nonlinear channel equalization and decoding using variational autoencoders," 2019, arXiv:1905.08795.
- [18] X. Yi, and C. Zhong, "Deep learning for joint channel estimation and signal detection in OFDM systems," 2020, arXiv:2008.03977.
- [19] E. Balevi, A. Doshi, A. Jalal, A. Dimakis, and J. G. Andrews, "High dimensional channel estimation using deep generative networks," 2020, arXiv:2006.13494.

- [20] W. F. Al-Azzo, B. M. Ali, S. Khatun, N. K. Noordin, and S. M. Bilfagih, "Peak-to-average power ratio reduction in OFDM systems using smoothing technique," in *Proc. IEEE 9th Malaysia Int. Conf. Commun.*, 2009, pp. 11–14.
- [21] Y. Jeon, H. Do, S. Hong, and N. Lee, "Soft-output detection methods for sparse millimeter-wave MIMO systems with low-precision ADCs," *IEEE Trans. Commun.*, vol. 67, no. 4, pp. 2822–2836, Apr. 2019.
- [22] Y. Suzuki and S. Narahashi, "Power amplifier configuration for Massive-MIMO transmitter," in *Proc. 22nd Asia-Pacific Conf. Commun.*, 2016, pp. 38–43.
- [23] X. Mao, Q. Li, H. Xie, R. Y. K. Lau, Z. Wang, and S. P. Smolley, "Least squares generative adversarial networks," in *Proc. IEEE Int. Conf. Comput. Vis.*, 2017.
- [24] S. Iizuka, E. Simo-Serra, and H. Ishikawa, "Globally and locally consistent image completion," *ACM Trans. Graph.*, vol. 36, no. 4, pp. 1–14, 2017.
- [25] J. Zhu, T. Park, P. Isola, and A. A. Efros, "Unpaired image-to-image translation using cycle-consistent adversarial networks," in *Proc. IEEE Int. Conf. Comput. Vis. (ICCV)*, 2017, pp. 2242–2251.
- [26] G. E. Hinton, N. Srivastava, A. Krizhevsky, I. Sutskever, and R. R. Salakhutdinov, "Improving neural networks by preventing co-adaptation of feature detectors," 2012, arXiv:1207.0580.
- [27] N. Srivastava, G. E. Hinton, A. Krizhevsky, I. Sutskever, and R. R. Salakhutdinov, "Dropout: A simple way to prevent neural networks from overfitting," *J. Mach. Learn. Res.*, vol. 15, no. 1, pp. 1929–1958, 2014.
- [28] W. C. Jakes, "Microwave mobile communications," Apr. 1992.
- [29] Y. Bengio, "Learning deep architectures for AI," *Found. Trends Mach. Learn.*, vol. 2, no. 1, pp. 1–127, Jan. 2009.